NON-DESTRUCTIVE PORE-SCALE APPROACH TO EVALUATE ELASTIC PROPERTIES OF SHALE SAMPLES BY IMAGING, MODELING AND SIMULATION

Weifeng Lv [1], Langqiu Flora Sun [2]
[1] Research Institute of Petroleum Exploration and Development, Beijing, China;
[2] China University of Petroleum, Beijing, China
This paper was prepared for presentation at the International Symposium of the Society of Core Analysts held in Trondheim, Norway, 27-30 August 2018

ABSTRACT
Elastic moduli are amongst the most important parameters to assess the shale plays and to instruct the hydraulic fracturing. However, due to extremely high brittleness of shale and very limited samples available, the conventional methods used to obtain elastic properties, such as uni-axial or tri-axial compression tests, often generate early breaking of shale samples, which leaves significant uncertainties on accurate evaluation of the elastic properties of shale samples. In this project, a new workflow to estimate the elastic moduli of shale samples is established with the aid of scanning electron microscopy (SEM) and numerical methods. A 2D mineralogical map of the external surface of a shale sample is obtained by Energy-dispersive X-ray spectra (EDS), from which not only the volumetric fraction but also the spatial correlation of each minerals is displayed. Finite element methods (FEM) are applied to this mineralogical map to simulate compression tests based on the principle of least elastic potential energy. Taking advantage of the flexibility of this simulation, anisotropy and other represented from the mineral map are also presented to clarify some aspects of the controversial debate on the representative volume of this work flow associated with its microscopic scale, and the potential upscale of the elastic properties from microscopic scale to core analysis scale. Also presented in this work are comparisons of the calculated elastic properties with some existing models that evaluate the effective moduli at macroscopic scales.

INTRODUCTION
Elastic moduli are important in the seismic exploration for shale gas, while at the same time and understanding of brittleness is crucial in finding sweet points for fracturing. Empirically the Young's modulus is positively related to brittleness. Thus, rock physicists are keen to measure elastic moduli of shale samples in order to determine Young's modulus. For conventional reservoir rocks, stress-strain experiments can be conducted. In contrast, core samples from promising shale gas reservoirs are usually too brittle for experimental studies. In addition, many shale gas reservoirs in China are deep, e.g. >2000 m, some even >4000 m. Drilling in such areas is extremely difficult and expensive, and well cores are precious.

Thanks to the development of scanning electron microscope (SEM), rock samples can be digitalized for virtual experiments without damaging the cores, i.e. digital core technique. This is potentially helpful for brittle shale. In most of the current studies, a core image is simply divided into pores and matrix (binary segmentation). This may be sufficient for sandstone, but mineral contents of shale are complicated and very significant. As a common example, the quartz-clay ratio largely determines shale brittleness. Thus, multi-phase segmentation is necessary.

There is always a concern on how a digital rock model based on images at the micron or millimetre scale can represent strata that are centimetre to metres in thickness. The key is to determine a representative size for the study purpose. Here we provide an analysis scheme and show the preliminary results of elastic properties of a shale sample that was generated by segmenting a pseudo-colour mineral map into multiple phases and simulating with finite-element method (FEM). The issue of defining a representative size is also investigated.

THEORY AND METHODS

In SEM, an incident electron beam stimulates energy-level transition of electrons of the atoms on a sample surface that results in the emission of characteristic X-rays. The analysis of the X-ray spectra yields elemental abundances, that in turn are transformed into mineral abundances. Applying this procedure on a point by point basis, a pseudo-colour mineral map was produced.

Instead of binary segmentation, we segmented a rock image into multiple phases: pores and minerals with larger volume fraction. Then the elastic properties are simulated by solving Hooke's law using a FEM scheme by Garboczi (1998). The principle is that the final elastic displacement under applied stress is such that the total energy stored is minimized, i.e.:

$$\frac{\partial E_n}{\partial u_m} = 0, \tag{1}$$

where *En* is elastic potential energy and u_m is elastic displacement at the *m*'th element. We have

$$E_n = \frac{1}{2} \iiint \left(\vec{\varepsilon} \cdot \vec{\vec{C}} \cdot \vec{\varepsilon} \right) dxdydz, \tag{2}$$

where $\vec{\varepsilon}$ and $\vec{\vec{C}}$ are the strain vector and elastic tensor at this element, respectively. By applying an initial stress, the strain and stress distribution at all the elements can be solved using an iterative approach. The effective elastic moduli can then be calculated.

In our application, the rock image is 2D and an element is a pixel of a single mineral. Isotropy is assumed at each pixel, so that $\vec{\vec{C}}$ can be calculated from the elastic moduli of

the mineral. Considering the relation among elastic moduli, any pair of moduli can be used, e.g., Young's modulus (E) and Poisson's ratio (ν), or bulk and shear moduli.

EXAMPLES AND RESULTS

The sample is black shale of upper Ordovician, acquired at a depth about 4400 m in a research well for shale gas prospecting in southeast rim of Sichuan Basin, China. Preliminary well logging and laboratory studies have been conducted. Well logs show relatively high fraction of total organic carbon (TOC), high brittleness index (BI), and low porosity (ϕ) at the stratum of the sample, namely SL5. Laboratory measurement gives a TOC fraction comparable to that in the well log. Table 1 compares the properties obtained from well logging ("log") and laboratory experiments ("lab").

Table 1. Rock properties of the SL5 sample

	ρ (g/cm^3)	TOC (wt.%)	BI (%)	ϕ (%)	E (GPa)	ν	Total gas content
logging	–	2.33	44.2	4.3	40.61	0.22	2.56
lab	2.645	2.27	–	–	–	–	3.13

Elastic properties (BI, ϕ, E, ν) are not measured in laboratory because the SL5 sample is too brittle for stress-strain experiment. In fact, only one stratum, SL3, in the entire well has laboratory results of elastic moduli. The SL3 is about 9 m below SL5, with E_{lab} = 33 GPa and ν_{lab} = 0.195. For comparison, E_{log} = 40.26 GPa and ν_{log} = 0.21 at SL3. Nevertheless, E_{lab} is obviously lower than E_{log}, implying that the SL3 sample has already been damaged due to brittleness before the experiment.

The SL5 sample is grinded and argon-ion polished before mounted into our SEM for back-scattering electron (BSE) images and mineral map. Figure 1 shows the sample before and after pre-processing.

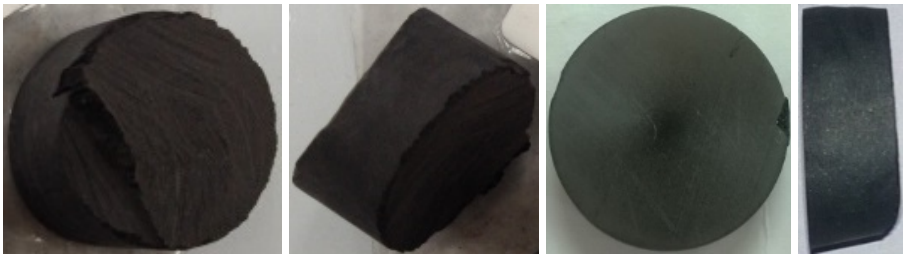

Figure 1. Photos of the SL5 sample, cylinder diameter 2.5 cm. Left to right: top view before pre-processing, side view before pre-processing, top view after pre-processing, side view after pre-processing.

BSE images of the sample have been produced at field of view (FOV) ranging from 488^2 to 14.2^2 μm^2 and resolution from 238.3 to 6.93 nm/pixel. Different types of pores can be observed: micro-fractures, inter-particle pores among clay minerals, intra-particle pores

in matrix grains, and organic pores. The numerous nano-scale pores greatly increase the adsorption area of methane molecules.

In general, grey shade in a BSE image is positively correlated to material density, which can be used for image segmentation. The ϕ and vol.% of kerogen are evaluated by counting "black" and "dark grey" pixels, respectively. We find that vol.% of kerogen are similar, about 2.2%, for images with FOV >170^2 μm^2, indicating that the sample can be regarded homogeneous at this extent, namely the representative size. That is, as long as the studying area is larger than this, the results can adequately represent the whole sample.

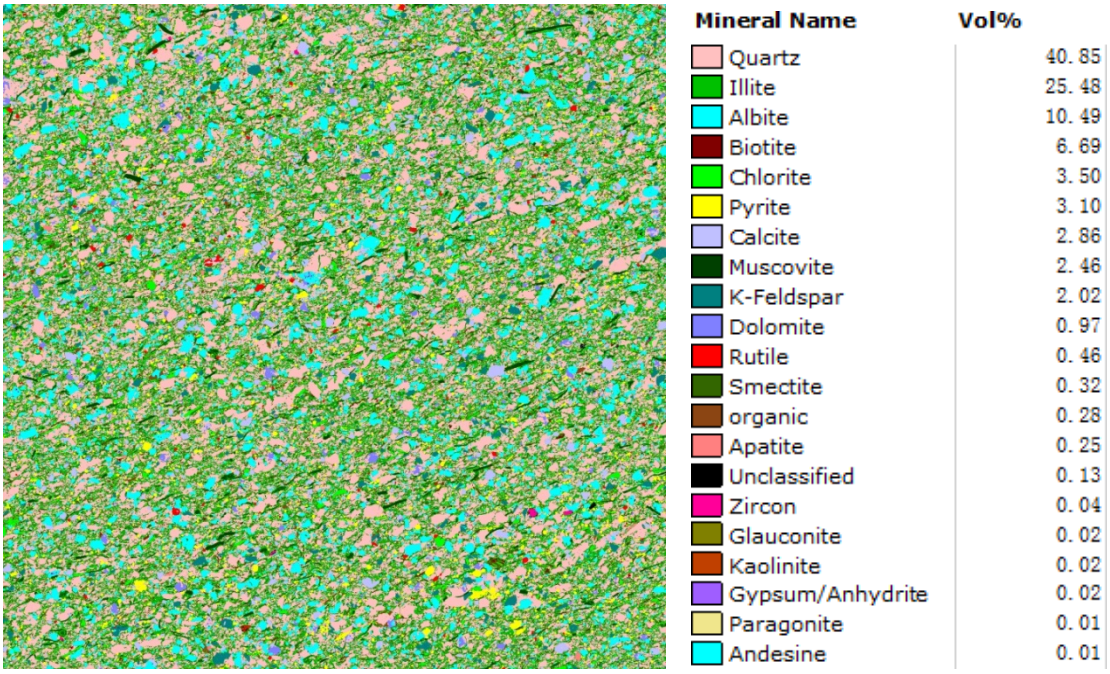

Figure 2. A pseudo-colour mineral map of the SL5 sample (left) and the mineral contents (right), using FEI QEMScan 650F, electron beam voltage 15 kV, FOV 1971×1977 μm^2, resolution 1 μm/pixel.

A limitation of BSE images is that various matrix minerals of shale with similar densities cannot be satisfactorily resolved. The pseudo-colour mineral map based on elemental spectra provides a way to separate the different minerals (Figure 2). The mineral map was then segmented into ten phases, the nine most abundant minerals with vol.% > 1% and pores. The rest minerals occupy 2.55% of the volume and are assumed to be pores. Considering the vol.% of kerogen in the BSE images, this assumption is reasonable. Table 2 lists the properties of the phases.

Table 2. Properties of the segmentation phases for Figure 2

Phase No.	1	2	3	4	5	6	7	8	9	0
Mineral	Quartz	Illite	Albite	Biotite	Chlorite	Pyrite	Calcite	Muscovite	K-feldspar	Pores
ρ (g/cm^3)	2.65	2.42	2.63	3.05	2.54	4.93	2.70	2.79	2.56	1.04
E (GPa)	94.5	38.6	69.0	33.8	118.5	305.9	81.6	77.4	72.1	0
v	0.07	0.24	0.35	0.36	0.25	0.15	0.29	0.25	0.28	0

Note: (1) Property data according to Mavko et al (2009), Mookherjee and Mainprice (2014).
(2) Pore density is calculated so that the density of whole image is 2.645 g/cm^3 as measured.

Figure 3 shows the segmentation with pores. Considering the representative size, a part of 600^2 μm^2 (see Figure 3) is used for FEM computing. Two cases of initial strain (ε) are tested: (1) stretching in x direction (ε_{xx} = 5‰, ε_{yy} = –0.35‰, ε_{xy} = 5‰), and (2) stretching in y direction (ε_{xx} = –0.35‰, ε_{yy} = 5‰, ε_{xy} = 5‰). Figure 4 compares the final stress (σ) distributions of the two cases. Stress concentration can be observed in the vicinity of pores. The calculated Young's moduli are 62.3 and 62.5 GPa, respectively; the calculated Poisson's ratios are 0.200 and 0.195, respectively. The results demonstrate isotropy of the sample.

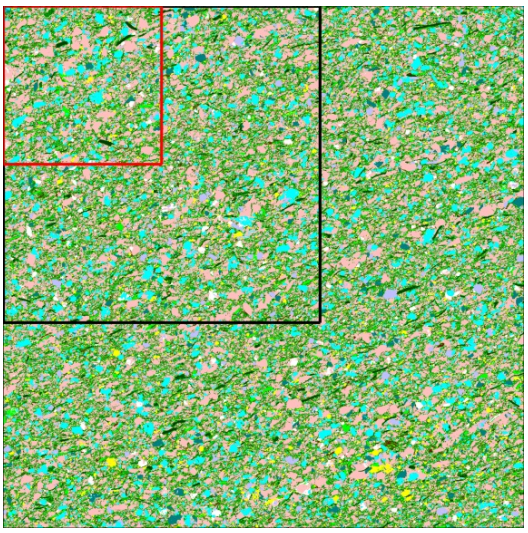

Figure 3. Segmentation and studying areas for FEM computing. White for pores, the other colours are the same as in Figure 2. Red and black boxes mark the 600^2 and 1200^2 μm^2 areas, respectively.

In Figure 2, vol.% of kerogen and ϕ are seriously underestimated compared to well log data and statistics on BSE images. The causes include: (1) most pores and kerogen areas are smaller than 1 μm, as shown in BSE images, e.g., organic pores; (2) voltage of the electron beam to produce the mineral map (15 kV) is higher than that for BSE images (10 kV), so that thin kerogen areas on the sample surface becomes transparent. Therefore, it

is important to combine different data types at different scales for comprehensive studies and reliable results.

The calculated Poisson's ratios all compare well with that in the well log. However, the calculated Young's moduli are systematically larger. This is possibly due to the scale of in situ fractures and high confining pressure in the original stratum; in addition, the measuring scales are different for well logging and laboratory studies.

Aware of the limitation of 2D simulation, our studies and results are preliminary. Further studies will focus on 3D modelling, e.g., how to reliably and effectively segment the matrix minerals of shale in 3D BSE images, and most importantly, how to represent a stratum with tiny digital rock models.

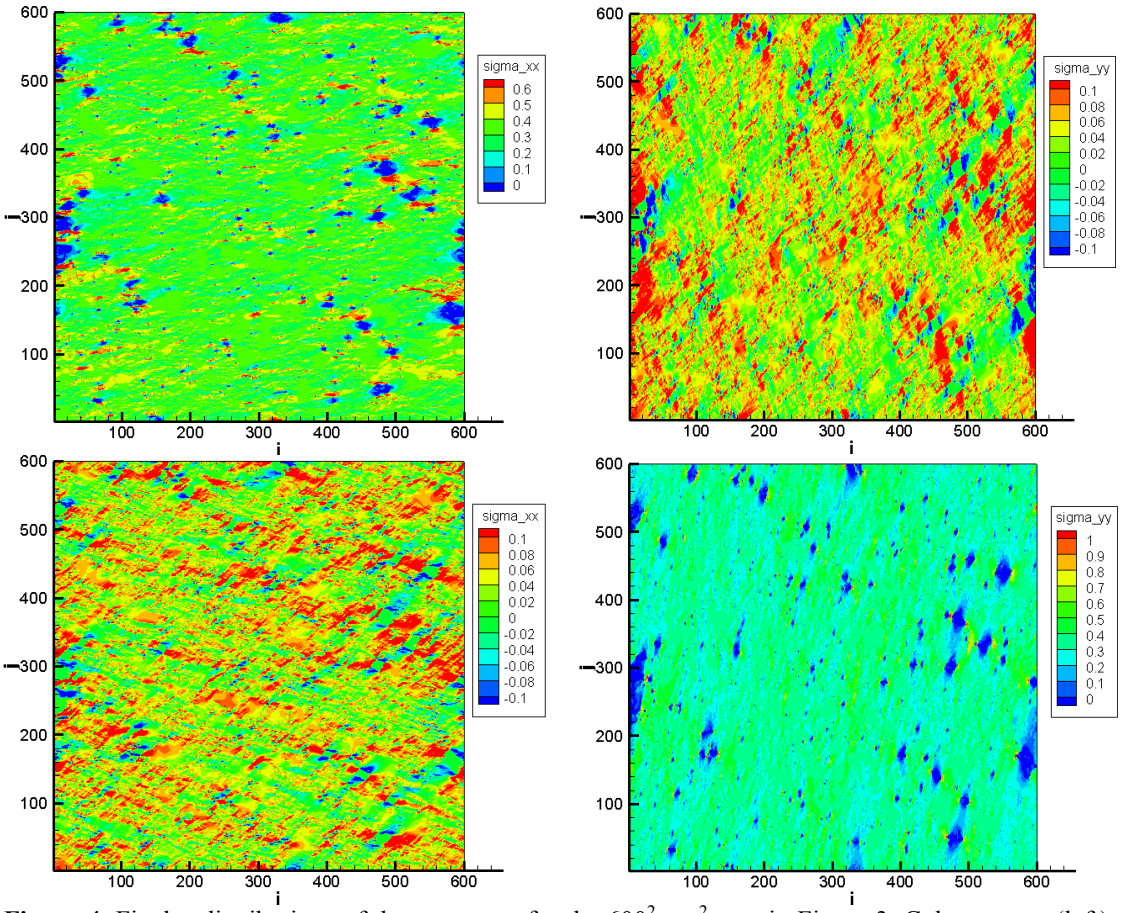

Figure 4. Final σ distributions of the two cases for the 600^2 μm^2 area in Figure 3. Columns: σ_{xx} (left) and σ_{yy} (right); rows: initial stretching in x (upper) and y (lower) directions. Colour-scale unit GPa.

CONCLUSION

Using a pseudo-colour mineral map produced by SEM and a FEM computing scheme, virtual stress-strain experiments can be conducted on a brittle shale sample, to which the laboratory experiment is not applicable. The key to proper elastic simulation of shale is

multi-phase segmentation instead of binary segmentation. By analysing a certain property (e.g., we use vol.% of kerogen) varying with image size, a representative size can be determined for the whole sample. Combining these techniques, the calculated Young's modulus and Poisson's ratio are reasonable and comparable to well log data.

REFERENCES

1. Garboczi, E.J. (1998): Finite element and finite difference programs for computing the linear electric and elastic properties of digital images of random materials. *National Institute of Standards and Technology*, USA, NISTIR 6269.
2. Mavko, G., T Mukerji, J. Dvorkin (2009): *The Rock Physics Handbook*, second edition. Cambridge University Press.
3. Mookherjee, M. and D. Mainprice (2014): Unusually large shear wave anisotropy for chlorite in subduction zone settings. *Geophysical Research Letters*, **41**, 1506-1513.
4. Garboczi, E. J., and A. R. Day. An Algorithm for Computing the Effective Linear Elastic Properties of Heterogeneous Materials: Three-dimensional Results for Composites with Equal Phase Poisson Ratios. *Journal of the Mechanics and Physics of Solids*. 1995.
5. Poutet J, Manzoni D, Hage-Chehade F, et al. The effective mechanical properties of random porous media. *Journal of the Mechanics & Physics of Solids*, 1996, 44(10):1587-1620.
6. Schlangen E, Garboczi E J. Fracture simulations of concrete using lattice models: Computational aspects. *Engineering Fracture Mechanics*, 1997, 57(2–3):319-332.
7. Wang M, Pan N. Elastic property of multiphase composites with random microstructures. *Journal of Computational Physics*, 2009, 228(16):5978-5988.
8. Roberts A P, Garboczi E J. Elastic properties of model random three-dimensional open-cell solids. *Journal of the Mechanics & Physics of Solids*, 2002, 50(1):33-55.